

Irreversible growth of binary mixtures on small-world networks

Julián Candia¹

¹*The Abdus Salam International Centre for Theoretical Physics,
Strada Costiera 11, 34014 Trieste, Italy*

Binary mixtures growing on small-world networks under far-from-equilibrium conditions are studied by means of extensive Monte Carlo simulations. For any positive value of the shortcut fraction of the network ($p > 0$), the system undergoes a continuous order-disorder phase transition, while it is noncritical in the regular lattice limit ($p = 0$). Using finite-size scaling relations, the phase diagram is obtained in the thermodynamic limit and the critical exponents are evaluated. The small-world networks are thus shown to trigger criticality, a remarkable phenomenon which is analogous to similar observations reported recently in the investigation of equilibrium systems.

PACS numbers: 05.70.Ln, 05.50.+q, 64.60.Cn, 75.30.Kz

I. INTRODUCTION

Complex networks are known to play a key role in the description of the structure and evolution of different mesoscopic and macroscopic systems. Indeed, the interacting parts of many natural and artificial systems can be interpreted as collections of linked nodes forming complex networks, whose structure and topology can be characterized in terms of statistical quantities such as their degree and path-length distributions, their connectivity, etc.

Empirical observations show that the mean distance between a pair of nodes within a connected real network is in general surprisingly short (typically of a few degrees and only logarithmically dependent on the system size), a phenomenon known as *small-world effect*. Moreover, the neighborhood of each node is observed to be, on average, highly interconnected [1].

The well-studied classical random graphs, which are networks built by linking nodes at random, display the small-world effect but have much lower connectivities than usually observed in real networks. In this context, the small-world networks were proposed few years ago [2, 3] as a realization of complex networks having short mean path-lengths (and hence showing the small-world effect) as well as large connectivities. Starting from a regular lattice, a small-world network is built by randomly adding or rewiring a fraction p of the initial number of links. Even a small fraction of added or rewired links provides the shortcuts needed to produce the small-world effect, thus displaying a global behavior close to that of a random graph, while preserving locally the ordered, highly connected structure of a regular lattice. Indeed, it has been shown that this small-world regime is reached for any given disorder probability $p > 0$, provided only that the system size N is large enough (i.e. $N > N_c$, where the critical system size is $N_c \propto 1/p$) [4, 5].

As a further step, recent works investigated the behavior of many standard models of Statistical Mechanics defined on small-world networks (as well as on other classes of complex networks) [1]. In particular, this was done for several equilibrium, Ising-type spin models. Generally

speaking, it was found that the structure and topology of the underlying complex networks affect dramatically the critical behavior of the models defined on them. For instance, it was found that the Ising model defined on a 1D small-world network presents a second-order phase transition at a finite critical temperature T_c for any value of the rewiring probability $p > 0$ [5, 6, 7]. Considering directed links, even the nature of the phase transition was found to change, switching from second to first order [8]. The ferromagnetic transition for the Ising model on small-world networks has also been studied numerically by rewiring 2D and 3D regular lattices [9].

Much less attention, however, has been devoted so far to the investigation of nonequilibrium transitions on complex networks. Some simple nonequilibrium models closely related to percolation were initially studied [10, 11, 12], while more recently a model for social interaction was investigated [13], in which the competition between dominance and spatial coexistence of different states in the nonequilibrium dynamics of Potts-like models was examined. Within the context of these recent developments, the aim of this work is to investigate the irreversible growth of binary mixtures on small-world networks.

The growth of a binary mixture (or, adopting an equivalent magnetic language, a two-state magnetic system of up and down spins) can be studied by means of the so-called magnetic Eden model (MEM) [14, 15, 16, 17, 18, 19], a natural generalization of the classical Eden model [20] in which the particles have an additional degree of freedom, the spin. Starting from a single seed, the growth takes place by adding, one by one, further spins to the immediate neighborhood (the perimeter) of the growing cluster, taking into account the corresponding interaction energies. By analogy to the Ising model, the energy E of a configuration of spins is given by

$$E = -\frac{J}{2} \sum_{\langle ij \rangle} S_i S_j, \quad (1)$$

where $S_i = \pm 1$ indicates the orientation of the spin for each occupied site (labeled by the subindex i), $J > 0$ is the ferromagnetic coupling constant between nearest-

neighbor (NN) spins, and $\langle ij \rangle$ indicates that the summation is taken over all pairs of occupied NN sites.

Setting the Boltzmann constant equal to unity ($k_B \equiv 1$) and measuring the absolute temperature T in units of J , the probability for a new spin to be added to the (already grown) cluster is defined as proportional to the Boltzmann factor $\exp(-\Delta E/T)$, where ΔE is the total energy change involved. At each step, all perimeter sites have to be considered and the probabilities of adding a new (either up or down) spin to each site must be evaluated. Using the Monte Carlo simulation method, all growth probabilities are first computed and normalized, and then the growing site and the orientation of the new spin are both determined by means of a pseudo-random number.

Although the configuration energy of a MEM cluster, given by Eq.(1), resembles the Ising Hamiltonian, it should be noticed that the MEM is a nonequilibrium model in which new spins are continuously added, while older spins remain frozen and are not allowed to flip.

The MEM has been studied extensively in regular lattices. The growth process of the MEM leads to an Eden-like self-affine growing interface and a fractal cluster structure in the bulk [14]. The existence of thermal order-disorder continuous phase transitions has been reported [16], as well as a rich variety of phenomena such as spontaneous magnetization reversals [17] and morphological [15], wetting [18] and corner wetting [19] transitions.

Here, a simple realization of small-world networks is adopted to investigate the growth of MEM clusters. Details on the model definition and the simulation method are given in Section 2. In Section 3, the behavior of the order parameter and the response functions of the system is studied and discussed. Remarkably, the order parameter distribution functions provide strong evidence for critical behavior arising from nonvanishing shortcut fractions in the network. Hence, the small-world network structure is shown to generate criticality in this nonequilibrium model for binary mixture growth, in analogy to similar phenomena observed recently in related equilibrium systems. Moreover, finite-size scaling is used to obtain a phase diagram showing the critical temperature as a function of the shortcut-adding probability of the network. A further quantitative characterization of the behavior of the system in the thermodynamic limit is provided by the determination of critical exponents. Finally, the conclusions of this work are presented in Section 4.

II. THE MODEL AND THE SIMULATION METHOD

Since the original rewiring-type model of Watts and Strogatz [2], different procedures to build small-world networks have been proposed. In this work, we adopt the one-dimensional, nearest-neighbor, adding-type small-world model [21]. In this realization, one starts with a ring of N sites and N bonds. Then, for each bond, a

shortcut (i.e. a link connecting a pair of randomly chosen sites) is added with probability p . In adding new links, multiple connections between any pair of sites are avoided, as well as connections of a site to itself. Since the original lattice bonds are not rewired, the resulting network remains always connected in a single component. On average, pN shortcuts are added and the mean coordination number is $\langle z \rangle = 2(1 + p)$. Note that p can also be regarded as the mean shortcut fraction relative to the number of fixed lattice bonds.

Once the network is created, a randomly chosen up or down spin is deposited on a random site. This first spin acts as the seed for the growth of the entire MEM cluster, following the rules described in the previous Section. As with other spin systems defined on complex networks, the magnetic interaction between any pair of spins is only present when a network bond connects their sites. The growth process naturally stops after the deposition of N particles, when the network becomes completely filled.

For any given set of defining parameters (i.e. the network size N , the shortcut-adding probability p and the temperature T), ensemble averages were calculated over 10^4 different (randomly generated) networks, and considering typically 50 different (randomly chosen) seeds for each network configuration. As explained in the Introduction, all normalized growth probabilities have to be recalculated at each deposition step. The resulting update algorithm is hence rather slow. Involving a considerable computational effort, this work presents extensive Monte Carlo simulations that cover the whole shortcut-adding probability range $0 \leq p \leq 1$ for different network sizes up to $N = 10^4$.

III. RESULTS AND DISCUSSION

The natural order parameter of a magnetic system is the total magnetization per site, i.e.

$$M = \frac{1}{N} \sum S_i, \quad (2)$$

which, in the context of this work, is to be measured on the completely filled network. However, since MEM clusters are grown from randomly chosen seeds, the ensemble average of the total magnetization is $\langle M \rangle \simeq 0$. Here, we will instead consider the absolute value of the total magnetization, $|M|$, as the order parameter, which is also appropriate to avoid spurious effects arising from finite-size spontaneous magnetization reversals [22, 23].

Figure 1 shows plots of $\langle |M| \rangle$ as a function of T , for different values of p and a fixed network size, $N = 100$. The effect of increasing p at a fixed temperature is that of increasing the net magnetization (and, hence, the order) of the system. Indeed, larger shortcut fractions favor long-range ordering connections between distant clusters across the network. Considering instead a fixed value of p , we see that, at low temperatures, the system grows ordered and the (absolute) magnetization is close to unity,

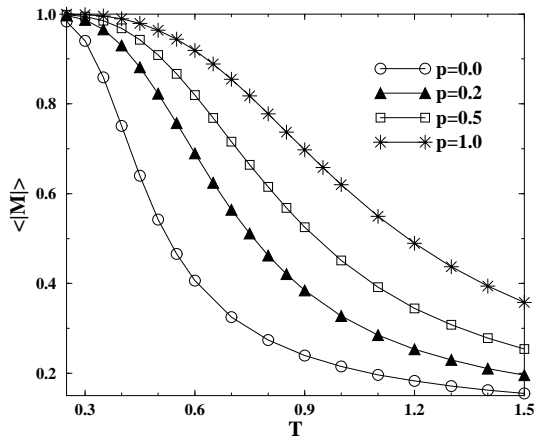


FIG. 1: Thermal dependence of the order parameter, for a fixed network size ($N = 100$) and different values of the shortcut-adding probability p , as indicated.

while at higher temperatures the disorder sets on and the magnetization becomes reduced significantly. However, fluctuations due to the finite network size prevent the magnetization from becoming strictly zero above the critical temperature, and the transition between the low-temperature ordered phase and the high-temperature disordered one becomes smoothed and rounded.

Strictly speaking, Figure 1 is just showing evidence of pseudo-phase transitions, which might be precursors of true phase transitions taking place in the ($N \rightarrow \infty$) thermodynamic limit. In the following, we will proceed to characterize in more detail this pseudo-critical state, by measuring other observables on finite-size systems. Further on, we will use standard finite-size scaling and extrapolation procedures to establish the phase diagram T_c vs p corresponding to the true phase transition in the thermodynamic limit, as well as to calculate critical exponents that describe the behavior of the system at criticality.

Let us now consider the magnetic susceptibility χ , given by

$$\chi = \frac{N^2}{T} (\langle M^2 \rangle - \langle |M| \rangle^2). \quad (3)$$

For equilibrium systems, the susceptibility is related to order parameter fluctuations by the fluctuation-dissipation theorem. Although the validity of a fluctuation-dissipation relation in the case of a nonequilibrium system is less evident, we will assume Eq.(3) to hold also for the MEM. Indeed, this definition of χ proves very useful for exploring the critical behavior of this system, as shown in earlier studies of the MEM in regular lattices [18, 19], as well as in other nonequilibrium spin models [24, 25].

Figure 2 shows plots of χ vs T , for different values of p and a fixed network size, $N = 100$. As with the thermal dependence of the order parameter shown in Figure

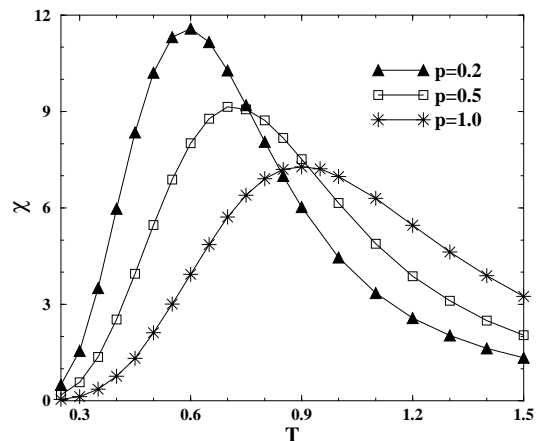


FIG. 2: Susceptibility as a function of the temperature, for different values of the shortcut-adding probability p and the fixed network size $N = 100$.

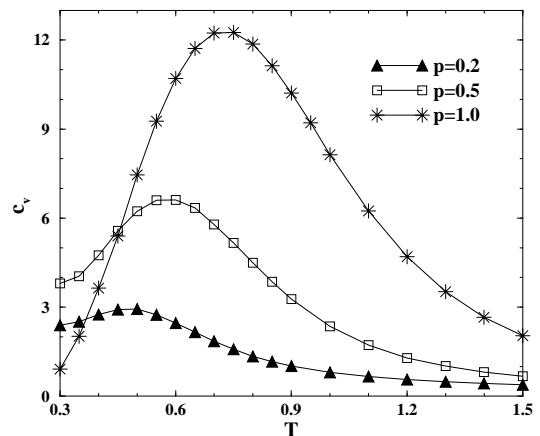


FIG. 3: Heat capacity per site as a function of the temperature, for a fixed network size ($N = 100$) and different values of the shortcut-adding probability p , as indicated.

1, the order-disorder transitions signaled by the peaks of the susceptibility become rounded and shifted. For a given probability p and system size N , we will define the “effective” finite-size critical temperature $T_c(N; p)$ as the temperature corresponding to the peak of the susceptibility. Although the transition temperature of finite systems is not uniquely and precisely defined, the susceptibility peaks become sharper as one considers larger systems, and the “effective” finite-size critical temperatures tend to the true critical temperature in the (infinite-size) thermodynamic limit [18, 22, 23].

In the same vein, the heat capacity per site can be related to energy fluctuations as

$$c_v = \frac{1}{NT^2} (\langle E^2 \rangle - \langle E \rangle^2). \quad (4)$$

Figure 3 shows plots of c_v vs T corresponding to the

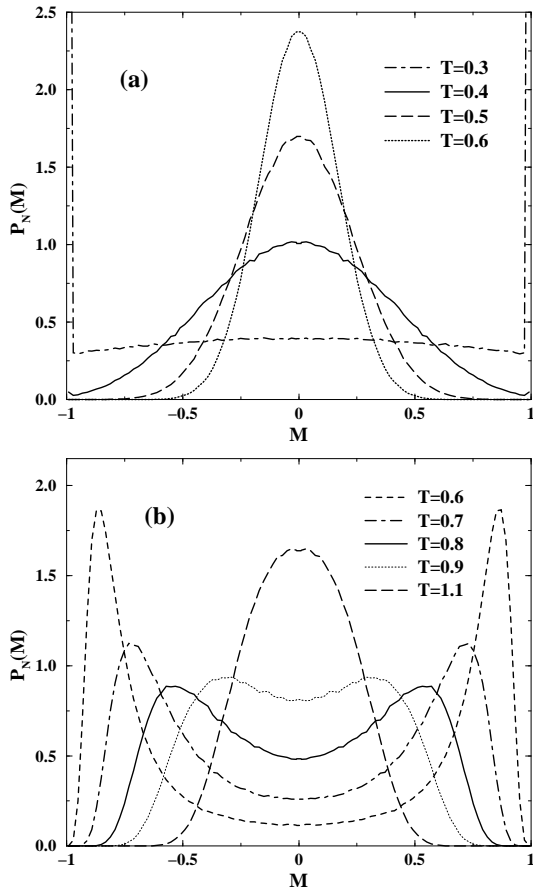


FIG. 4: Normalized probability distributions of the magnetization, for a fixed lattice size ($N = 1000$) and different temperatures, as indicated. (a) The ($p = 0$) regular lattice, which exhibits local or absolute maxima at $M = 0$ (the fully disordered state) and $M = \pm 1$ (the completely ordered states). The sharp peaks at $M = \pm 1$ for $T = 0.3$ have been truncated. (b) The small-world network with shortcut-adding probability $p = 0.5$. The gradual onset of maxima at $M = \pm M_{sp}$ ($0 < M_{sp} < 1$) across the transition, which become sharper and approach $M = \pm 1$ as T is decreased, is the hallmark of a true thermally-driven continuous phase transition. See more details in the text.

same parameter values used before. Compared to the susceptibility, the heat capacity exhibits flatter shapes and broader peaks.

Further insight can be gained by examining the normalized probability distribution of the magnetization, $P_N(M)$. Fixing the network size ($N = 1000$), the behavior of $P_N(M)$ for different temperatures is shown in Figure 4 for (a) the regular lattice and (b) the small-world network with shortcut-adding probability $p = 0.5$. For high temperatures, in both cases the probability distributions are Gaussian-shaped and centered at $M = 0$, as expected for thermally disordered systems. However, their behavior is remarkably different at intermediate and low temperatures.

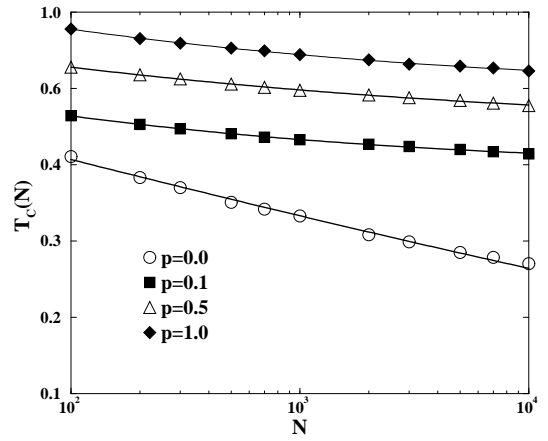


FIG. 5: Effective transition temperatures $T_c(N)$ for $10^2 \leq N \leq 10^4$ and different values of p , as indicated. Fits to the data using the finite-size scaling relation, Eq.(5), are also shown.

For $p = 0$ (see Figure 4(a)), the curvature of the distribution is convex and exhibits a local maximum always situated at $M = 0$, while other maxima develop at $M = \pm 1$. At very low temperatures, the curved shape flattens and the maxima at $M = \pm 1$ dominate the distribution. Irrespective of the temperature, neither absolute nor local maxima arise at any intermediate values of the magnetization, i.e. different from $M = 0$ (the fully disordered state) and $M = \pm 1$ (the completely ordered states). In fact, this noncritical behavior is in agreement with previous results for the MEM in the lattice: a cluster growing in a linear or planar regular lattice from a single seed shows only a pseudo-phase transition with a “critical” temperature $T_c(N)$ that vanishes in the ($N \rightarrow \infty$) thermodynamic limit [14]. An analogous behavior was observed in the MEM grown in a stripped (1+1)-dimensional rectangular geometry using linear seeds [16]. Only in higher dimensional stripped geometries true critical phase transitions have been reported [16, 18].

In contrast, in the small-world network (see Figure 4(b)) one observes the onset of two maxima located at $M = \pm M_{sp}$ ($0 < M_{sp} < 1$), which become sharper and approach $M = \pm 1$ as T is gradually decreased. The smooth shift of the distribution maxima across $T \simeq T_c$, from $M = 0$ to the low-temperature nonzero spontaneous magnetization $M = \pm M_{sp}$, is the signature of true thermally-driven continuous phase transitions [16, 23]. Hence, critical behavior in the irreversible growth of MEM clusters arises from the presence of shortcuts in the small-world network. This remarkable result is a nonequilibrium realization of analogous phenomena observed in related equilibrium systems, as e.g. the Ising model in small-world networks generated from rewiring 1D lattices [5, 6, 7].

In order to explore further this phenomenon, we will

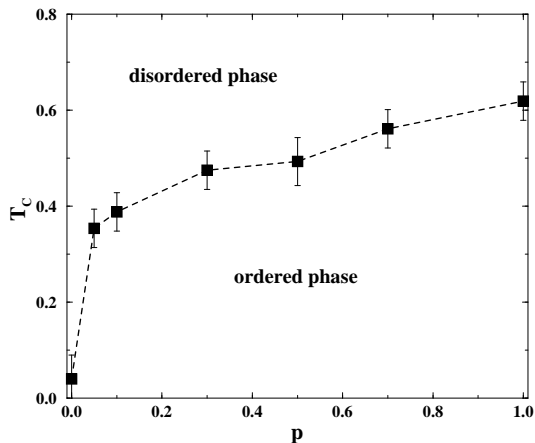


FIG. 6: Phase diagram T_c vs p in the $(N \rightarrow \infty)$ thermodynamic limit. The MEM growing on small-world networks with any value of $p > 0$ undergoes thermally-driven continuous phase transitions. In the regular lattice limit, $p = 0$, the system is noncritical. The dashed line is a guide to the eye.

extrapolate the finite-size “critical” temperatures to the thermodynamic limit and build the corresponding phase diagram, in which the critical temperature is given as a function of the shortcut-adding probability of the network. Moreover, this procedure will also allow to determine the critical exponents of the system.

According to the finite-size scaling theory, developed for the treatment of finite-size effects at criticality and under equilibrium conditions [26, 27], the difference between the true critical temperature, T_c , and the effective pseudo-critical one, $T_c(N)$, is given by

$$|T_c - T_c(N)| \propto N^{-1/\nu}, \quad (5)$$

where ν is the exponent that characterizes the divergence of the correlation length at criticality.

Figure 5 shows the effective transition temperatures for different network sizes in the range $10^2 \leq N \leq 10^4$ and different shortcut fractions, together with the corresponding finite-size scaling fits. Clearly, Eq.(5) provides an excellent fit to all the data.

Figure 6 shows the extrapolated phase diagram T_c vs p . As anticipated, for $p > 0$ the system undergoes critical order-disorder phase transitions at finite critical temperatures: the small-world network geometry triggers criticality. Naturally, the global ordering imposed by long-range shortcuts is weaker the lower the shortcut fraction, and hence T_c decreases monotonically with p . The critical temperature vanishes for $p = 0$, which is the expected regular lattice limit behavior.

The same fitting procedure also determines the critical exponent ν . The obtained value is $\nu = 3.6 \pm 0.4$.

An additional characterization of the critical behavior of this system can be obtained by calculating the critical exponent γ , which describes the divergence of the susceptibility at the critical point. Using again the finite-size

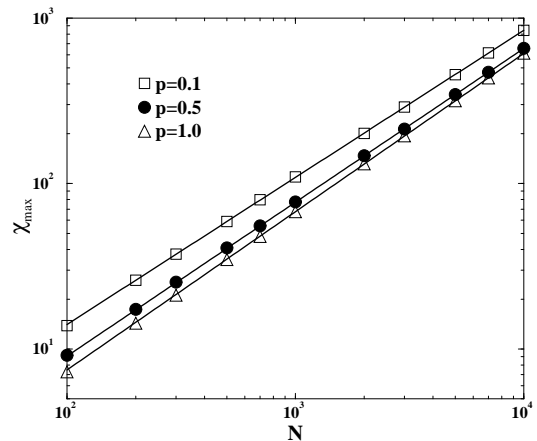


FIG. 7: Plots showing the maxima of χ for different network sizes in the range $10^2 \leq N \leq 10^4$ and different shortcut fractions. Also the corresponding finite-size scaling fits, given by Eq.(6), are shown for comparison.

scaling theory, the exponent ratio γ/ν can be related to the peak of the susceptibility measured in finite samples of size N by

$$\chi_{max} \propto N^{\gamma/\nu}. \quad (6)$$

Figure 7 shows the maxima of χ plotted against the network size for different values of p , as indicated. Fits to the data using this scaling relation are also shown. It turns out that $\gamma/\nu = 0.92 \pm 0.04$. Using this ratio and the value already obtained for ν , we determine $\gamma = 3.3 \pm 0.4$.

IV. CONCLUSIONS

Binary mixtures growing irreversibly on small-world networks are studied numerically by means of extensive Monte Carlo simulations performed on the magnetic Eden model. Firstly, evidence for the occurrence of order-disorder pseudo-phase transitions is provided by the order parameter and the response functions of finite samples. Then, studying the order parameter distribution functions, a clearly different behavior between the noncritical regular lattice ($p = 0$) and the small-world network ($p > 0$) is observed. Indeed, the latter shows the behavior expected for systems undergoing thermally-driven continuous phase transitions. Hence, it is concluded that a small fraction of shortcuts is sufficient to trigger criticality.

In order to obtain additional evidence of this phenomenon, standard finite-size scaling relations are used to determine the phase diagram T_c vs p , in which the critical temperature is shown as a function of the shortcut-adding probability of the network. As expected, for $p > 0$ the system undergoes order-disorder continuous phase transitions at finite critical temperatures. Since the long-range ordering is weaker the lower the shortcut fraction,

T_c decreases monotonically with p and vanishes for $p = 0$. Moreover, the behavior of the system at criticality is further characterized by the calculation of the critical exponents $\nu = 3.6 \pm 0.4$ and $\gamma = 3.3 \pm 0.4$.

These results, obtained in the framework of nonequilibrium growth systems, are a novel realization of analogous phenomena, which have recently been reported in the investigation of equilibrium systems. The present work will thus hopefully stimulate and contribute to fur-

ther developments in the fields of complex networks and nonequilibrium statistical physics.

Acknowledgments

The author thanks Ezequiel V. Albano, Ginestra Bianconi, and Simona Rolli for useful discussions.

-
- [1] S. N. Dorogovtsev and J. F. F. Mendes, *Evolution of Networks* (Oxford University Press, New York, 2003).
 - [2] D. J. Watts and S. H. Strogatz, *Nature* **393**, 440 (1998).
 - [3] D. J. Watts, *Small Worlds* (Princeton University Press, Princeton, 1999).
 - [4] M. E. J. Newman and D. J. Watts, *Phys. Lett. A* **263**, 341 (1999).
 - [5] A. Barrat and M. Weigt, *Eur. Phys. J. B* **13**, 547 (2000).
 - [6] M. Gitterman, *J. Phys. A: Math. Gen.* **33**, 8373 (2000).
 - [7] A. Pekalski, *Phys. Rev. E* **64**, 057104 (2001).
 - [8] A. D. Sánchez, J. M. López, and M. A. Rodríguez, *Phys. Rev. Lett.* **88**, 048701 (2002).
 - [9] C. P. Herrero, *Phys. Rev. E* **65**, 066110 (2002).
 - [10] M. Kuperman and G. Abramson, *Phys. Rev. Lett.* **86**, 2909 (2001).
 - [11] R. Pastor-Satorras and A. Vespignani, *Phys. Rev. Lett.* **86**, 3200 (2001).
 - [12] V. M. Eguíluz and K. Klemm, *Phys. Rev. Lett.* **89**, 108701 (2002).
 - [13] K. Klemm et al., *Phys. Rev. E* **67**, 026120 (2003).
 - [14] M. Ausloos, N. Vandewalle, and R. Cloots, *Europhys. Lett.* **24**, 629 (1993); N. Vandewalle and M. Ausloos, *Phys. Rev. E* **50**, R635 (1994).
 - [15] J. Candia and E. V. Albano, *Eur. Phys. J. B* **16**, 531 (2000).
 - [16] J. Candia and E. V. Albano, *Phys. Rev. E* **63**, 066127 (2001).
 - [17] J. Candia and E. V. Albano, *J. Appl. Phys.* **90**, 5395 (2001).
 - [18] J. Candia and E. V. Albano, *Phys. Rev. Lett.* **88**, 016103 (2002); *J. Phys.: Cond. Matt.* **14**, 4927 (2002); *J. Chem. Phys.* **117**, 6699 (2002).
 - [19] V. Manías, J. Candia, and E. V. Albano, *Eur. Phys. J. B* **47**, 563 (2005).
 - [20] M. Eden, *Symposium on Information Theory in Biology*, H. P. Yockey (Ed.) (Pergamon Press, New York, 1958); *Proc. 4th Berkeley Symposium on Mathematics, Statistics and Probability*, F. Neyman (Ed.) (University of California Press, Berkeley, 1961), Vol. IV, 223.
 - [21] M. E. J. Newman and D. J. Watts, *Phys. Rev. E* **60**, 7332 (1999).
 - [22] D. P. Landau and K. Binder, *A guide to Monte Carlo simulations in Statistical Physics* (Cambridge University Press, Cambridge, 2000).
 - [23] K. Binder and D. W. Heermann, *Monte Carlo simulation in statistical physics: an introduction, 4th ed.* (Springer-Verlag, Berlin, 2002).
 - [24] S. W. Sides, P. A. Rikvold, and M. A. Novotny, *Phys. Rev. Lett.* **81**, 834 (1998); *Phys. Rev. E* **59**, 2710 (1999).
 - [25] G. Korniss et al., *Phys. Rev. E* **63**, 016120 (2001).
 - [26] M. N. Barber, *Phase transitions and critical phenomena*, C. Domb and J. L. Lebowitz (Eds.) (Academic, New York, 1983), Vol. 8.
 - [27] V. Privman (Ed.), *Finite size scaling and numerical simulations of statistical systems* (World Scientific, Singapore, 1990).